

СООБЩЕНИЯ
ОБЪЕДИНЕННОГО
ИНСТИТУТА
ЯДЕРНЫХ
ИССЛЕДОВАНИЙ

Дубна

96-96

E9-96-96

V.B.Kutner, S.L.Bogomolov

MULTIPLY-CHARGED HEAVY ION SOURCE
FOR GASEOUS AND SOLID MATERIALS

1996

I. INTRODUCTION

The PIG ion source with indirectly heated cathode is capable to produce the intense beams of multiply charged ions ($z < 10$) of gases and solids up to uranium. This ion source was developed for acceleration of multiply charged ions at cyclotrons and then at linear accelerators for the experiments in fundamental nuclear physics. It is also used at the high energy implanters. Owing to long-term study of this source in many centers the highly charge states of Xe up to 15 (50 mA) and intense beams of low charge states (~ 100 mA) were achieved. In the present paper the results of investigations of the PIG source which could be useful for technology applications are presented.

II. GENERAL ASPECTS

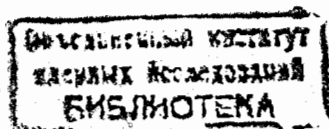
The ion source described below is used for the production of accelerated multiply charged ions of gaseous and solid materials at the FLNR JINR cyclotrons [1]. The schematic view of the ion source head is shown in Fig.1. The diagram of the power supply circuit is shown in Fig.2. The discharge chamber (3) of the source is placed in the gap of the electromagnet. The ions are extracted through the emission slit (5) across the magnetic field direction by applying the high voltage between the discharge chamber and the extractor electrode. For production of ions of solid materials the electrode (4) with the working material contained therein is used. This electrode is fastened on a movable insulated water-cooled holder. The position of the electrode and the potential applied to it are regulated for the optimal operating conditions to be established. For production of multiply-charged ions at cyclotrons the following modes of operation are frequently used:

- the pulsed discharge current of 5 - 15 A
- the pulsed discharge voltage of 400 - 1200 V
- the cathode heating power of 0,5 - 1 kW
- the pulse length of 1 - 3 ms
- the repetition rate of 100 - 150 Hz.

As a rule the cross-section of the discharge chamber is 8×8 mm², and the dimension of the emission slit is 2×15 mm². The distance between the cathode and anticathode in the ion sources used at the cyclotrons is from 45 up to 220 mm. The consumption of gas depends on its mass and the discharge mode and typically ranges from 0,15 sccm for Xe up to few sccm for He. The consumption of solid materials and also the potential and current of the sputtering electrode greatly depend on the sputtering material properties (melting point, coefficient of sputtering, conductivity and so on). In routine operation the consumption of solid materials is about 10 - 20 mg/hour.

Below, some results, obtained with such ion source at test bench operation are presented. The test bench represents the Dempster type mass-spectrometer. At test bench operation the ion source works in the magnetic field 0,3 - 0,4 T in pulsed mode with the pulse length of 1 ms and repetition rate of 100 Hz. The extraction voltage equals 15 - 25 kV. The dimension of the emission slit is 1×15 mm². The total extracted currents are of the order of magnitude of 100 mA in pulse. In Table I the yield of different ions of solid materials are presented [2]. The currents of all charge states of solid ions and their percentage in the total extracted current are also indicated in the Table I. The Table II represents the yield of ions of gases in test bench operation.

In Fig.3 the yield of ions of different mass with a given mass (A) to charge (Z) ratios ($A/Z=10 - 20$) produced at test bench is given.



III. EFFECT OF EMISSION SURFACE ENLARGEMENT

The current density of extracted ions is proportional to the electron temperature and plasma density [3]. The increase of the total extracted current can be achieved by the enlargement of the plasma emission surface.

The operation of the PIG ion source with various dimensions of the extraction slits was tested at the JINR FLNR cyclotrons [4]. In this experiments the available dimensions of the extraction slit were bounded by the configuration of the cyclotron accelerating system. It was shown, that the current of accelerated beam increases with the increase of the emission slit area. The increase of the slit length is more effective for production of more intense accelerated ion beam that is probably dealt with the features of the cyclotron accelerating system.

The experiments the other authors show practically the linear increase of the extracted current with the area of the emission slit [5,6].

On the FLNR JINR test bench the operation of the source with several slits was tested. In Fig.4 the scheme of experiment with two extraction slits situated on the opposite walls of discharge chamber is shown. The mode of source operation was chosen usual for cyclotron. The ions were extracted by d.c. voltage up to 20 kV. One of the slits could be open (or closed) to provide the simultaneous extraction from both or one of the slits. The investigation showed that the total extracted current and charge state distribution of the ion beam extracted from the one of the slits is not affected by the simultaneous extraction of ions from the other slit. The additional emission slit requires insignificant increase (about 20%) of gas consumption to keep the other parameters of discharge. The intensities of the ion beams extracted in opposite directions are comparable.

The ion source with several emission slits and extended cathode was also tested. The extended cathode has the dimensions $7 \times 14 \text{ mm}^2$, the cross-section of the discharge chamber equals $8 \times 16 \text{ mm}^2$. The scheme of the experiment is shown in Fig.5. The emission slits could be closed or open during the source operation realizing the one- two- or three-slits version. To provide the extraction and analysis of the ion beam from the different points of discharge in the median plane, the extraction electrode could be moved parallel to the plate with emission slits.

In case of the extended cathode the heating power of the cathode should be increased by factor 1.5. If the additional emission slits are open the gas consumption should be increased up to 30%. The investigations showed that the intensities of the beams extracted from each of the emission slits are comparable. The extraction of the beam from the lateral slits does not affect the charged state distribution of ions extracted from the central slit.

In Fig.6 the sketch of the discharge chamber with circular slit is shown. The circular slit (3mm in height) could be partly closed by the movable cylinder at ground potential, so the beam could be extracted from the slit $2,5 \times 3 \text{ mm}^2$ only, or from the circular slit by the circular extraction electrode with simultaneous analysis of the part of the extracted beam. The results are shown in Table III, where the charge state distributions of Xe ions for both cases are presented.

The experiments were made with the discharge mode 11 A, 800 V in pulse, pulse duration 1 mS, repetition rate - 100 Hz. Working gas - Xe, magnetic field strength - 3,6 kGs, extraction voltage - 17 kV.

The above mentioned experiments show various ways of increasing the emission surface of the PIG source. The increase of the emission surface does not change the charge state distribution of ions extracted from the source.

IV. SPATIAL DISTRIBUTION OF MULTIPLY CHARGED IONS IN THE DISCHARGE COLUMN

The spatial distributions of the multiply charged ions along the discharge column and in transverse direction are important from the point of view of possible emission surface enlargement. The spatial distribution of the multiply charged ions inside the source can be characterized by the data of spectrometric measurements. Fig.7 [7] shows the distribution of the Ar spectral lines intensity along the discharge chamber. The decrease of the Ar lines intensity in the cathode and anticathode regions is caused by the influence of the sputtered atoms of the cathode and anticathode. The direct measurements of the charge state distribution of ions, extracted from the slits arranged at different positions along the discharge were fulfilled by Dr. B.N.Makov [8]. Fig.8 illustrates the scheme of the experiment and the charge state distribution of Xe ions. The results of this experiment accord with the data of spectrometric measurements.

The spatial distribution of multiply charged ions in the ion source with Mo sputtering electrode and Xe as a support gas was measured by Dr. Yu.P.Tretyakov [9]. Fig.9 shows the distribution of $\text{MoV}(\text{Mo}^{4+})$ spectral line intensity along the discharge. The dashed lines indicate the dimensions of the sputtering electrode. It is seen that the intensity is nearly constant within the sputtering electrode boundaries and sharply decreases outside. It means that the sputtering electrode should be introduced into the discharge chamber on a level of emission slit and its height should corresponds to that of a slit. The transverse distribution of Mo and Xe spectral lines is shown in Fig.10. The spectral lines of neutral and singly charged Mo ions are seen near the sputtering electrode surface only. It means that for reducing the flux of neutrals from the source the sputtering electrode should be displaced relatively far from the emission surface, for example on the opposite wall of the discharge chamber.

The spectrometric measurements show that the increase of the emission surface in longitudinal direction is bounded by the dimensions of the discharge zone free of ions of cathode and anticathode materials. On the other hand, the presence of ions of cathode and anticathode materials in the discharge can be used for production of plasma containing such ions. For this purpose the design of the source should be changed for proper disposition of anticathode and emission surface.

V. PRODUCTION OF MULTIPLY CHARGED IONS OF REFRACTORY METALS

Basing on the results of spectrometric measurements of Mo ions distribution as a function of the distance from the anticathode [10] and experiments on production of W ions in the gaseous ion source [11] the modified version of the source for production of multicharged ions of refractory metals was designed and tested.

The schematic view of the source is shown on Fig.11. The anticathode is situated in the extraction slit region. The distance between the median plane and the working surface of the anticathode was determined as 15 mm for optimal yield of W^{10+} ions. The ion source was tested at the test bench and the charged state distributions of extracted ions were investigated. The ions were extracted from the emission slit $1 \times 20 \text{ mm}^2$. For production of Mo and W ions the ion source was ignited on Kr or Xe. The ion currents produced in operation with Mo and W anticathodes are presented in Table IV. For comparison, the intensities of the beams produced in the ion source with sputtering electrode are also presented. It is seen that due to cathode sputtering of the anticathode more intense ion beams in comparison with the data presented in Table I are produced. The maximum in the charge state distribution is shifted towards the higher charges.

Table I. Solid states ion yield from the PIG source at test operation

Element	Discharge		Regime Sputtering		Support gas	Ion yield (mA/peak)											Total current mA	Conditions of analysis		
	U _d , V	I _d , A	U _s , V	I _s , A		1+	2+	3+	4+	5+	6+	7+	8+	9+	10+	11+		12+	%	H ₁ , KG
Z																				
12 Mg	660	7.5	520	2.9	Ar	18	85	32	3.0	0.4	0.06	0.005					140	77	3.6	15
13 Al	300	8.2	980	1.9	Xe	22	59	20	3.4	0.25	0.04						105	95	3.6	15
14 Si	620	11	1900	2.5	Xe	12	46	35	13	1.6	0.18	0.018					104	80	3.6	24
15 P	1000	5.3	1000	1.0	Ar	3	6.3	5.5	1.2	0.26	0.03						16	18	3.6	17
20 Ca	600	9.5	540	1.8	Xe	3	23	22	14	4.5	1.0	0.18	0.035				66	60	3.6	17
21 Se	500	8	1700	0.64	Xe	1.3	18	19	4.9	0.8	0.05	0.01					45	74	3.6	17
22 Ti	750	16	1250	2.4	Xe	2.1	8.5	14	14	8.8	1.1	0.33	0.035				43	43	4.4	21
23 V	900	15	1400	1.6	Xe	6.3	19	12	14	6.4	1.1	0.15	0.03				59	74	4.4	22
24 Cr	1200	15	850	1.0	Xe	3.7	11	5.2	10	8.8	3.3	0.55	0.06	0.002			48	63	4.4	21
25 Mn	650	8.5	800	0.7	Xe	5	16	18	11.3	6.1	1.6	0.39	0.09	0.026	0.001		56	83	4.4	20
26 Fe	480	13	600	1.6	Xe	3	13	14	6.4	1.7	0.33	0.12	0.04	0.004			38	76	5.3	25
27 Co	500	15	790	1.3	Xe	13	19	15	10	2.5	0.83	0.06	0.01	0.002			59	70	3.6	17
28 Ni	800	6	1000	1.0	Xe	-	23	24	16	6.7	1.5	0.44	0.08	0.03			73	60	3.6	17
29 Cu	540	10	400	2.3	Ar	-	30	32	35	26	6.6	1.9					150	70	3.6	17
30 Zn	400	7.5	560	1.6	Xe	-	70	55	29	9.5	3.95	0.76	0.2	0.024			170	93	3.6	15
32 Ge	900	5.5	2000	0.5	Ar	8.4	17	9.5	11	6.4	1.35	0.48	0.09				54	77	3.6	20
34 Se	950	10	500	0.65	Xe	-	3.9	9.5	7.6	5.8	1.35	0.56	0.18	0.01			29	32	5.3	22
40 Zr	1100	5	1100	0.8	Ar	-	6.9	4.1	5.9	3.72	1.41	1.0	0.47	0.15	0.04		24	34	3.6	16
41 Nb	700	20	880	1.6	Xe	0.7	4.8	6.8	11	17.3	3.8	1.1	0.33	0.044	0.004		29	45	4.4	24
42 Mo	380	9.5	940	1.8	Xe	-	24	25	23	16.8	9.4	2.0	0.4				100	90	3.6	15
48 Cd	900	10	200	1.0	Ar	-	14	18	28	37	22	11.3	3	0.74	0.11	0.025	146	90	4.4	20.5
49 In	540	11	1250	0.65	Ar	-	1.7	3.3	6.4	7.4	4.4	3.2	1.2	0.33	0.018		29	65	5.3	26
50 Sn	840	11	550	0.75	Xe	-	1.6	2.6	3.3	2.9	3.0	3.7	1.3	0.13			18	40	4.5	22
57 La	760	11	850	1.1	Xe	-	8.5	7.7	7.9	5.5	5.0	3.3	2.0	0.9	0.042		57	57	4.4	20
72 Hf	650	7	750	1.0	Ar	3.9	4.1	3.6	4.5	4.71	2.33	0.6	0.21	0.05	0.01		24	72	5.3	18
73 Ta	470	9.8	970	1.5	Ar	-	-	11.4	18.9	12.5	8.4	3.0					54	65	3.6	15
74 W	360	9	980	1.4	Xe	-	-	20	17.1	13.1	6.8	3.3	0.7	0.12			61	65	3.6	15
75 Re	580	20	540	2.8	Ar	-	15	14	12.4	14.3	8.6	6	0.9	0.6			86	66	3.7	18
82 Pb	950	10	500	0.65	Xe	-	-	1.3	4.9	5.5	8.95	8.8	7	3.9	2.1		42	46	5.3	22
83 Bi	860	8.5	480	0.5	Ar	-	-	2.4	2.8	5.6	6.3	4.2	2.0	1.2	0.91	0.22	30	55	3.6	17
90 Th	1200	10	750	0.9	Ar	-	-	1.6	4.3	8.6	6.8	1.5	1.8	1.8	1.2	4.8	89	53	5.3	17

TABLE II. Gases ion yield from the PIG source at test operation (mA/peak)

Z	1+	2+	3+	4+	5+	6+	7+	8+	9+	10+	11+	12+	13+	14+	15+
N ₂	19	16	9.7	0.9	0.03										
O ₂	42	19	9.1	1.7	0.04										
Ne	36	28	10	1.2	0.12										
Ar	25	28	35	12	10	2.8	1.2	0.2							
Kr			25	14	10	13*	6.0	3.7	1.1						
Xe			27	18	16	14	16	20*	9.1	.12	.015	0.8	0.14	0.06	0.01

* including spurious ions

TABLE III

Charge state distribution of Xe ions extracted from the source with circular emission slit

Circular slit	Ion yield (mA/peak) / % of the total current									
	1+	2+	3+	4+	5+	6+	7+	8+	9+	10+
closed I _t = 20 mA	0,5	1.0	3.9	3.2	3.4	2.5	1.6	0.9	0.4	0.075
	2.4	4.8	19	16	17	12	8	4.3	2	0.4
open I _t = 150 mA	2.5	5	20	21	17	11	4.6	14*	1	0.2
										%

(*) - including spurious ions

TABLE IV. Mo and Ta ion yield from the modified ion source and from the source with sputtering electrode

Metal	Discharge mode		Ion yield (mA / peak)										
	I _d , A	U _d , V	1+	2+	3+	4+	5+	6+	7+	8+	9+	10+	
Mo	14	530		24					10	9	2.4	0.6	0.05
*	9.5	380		24	24	23	16	9.4	2.0	0.4			
W	14	500					5	18	36	30	13	9	
*	9	360			20	17	13	6.8	3.3	0.7	0.12		

* - data for the ion source with sputtering electrode

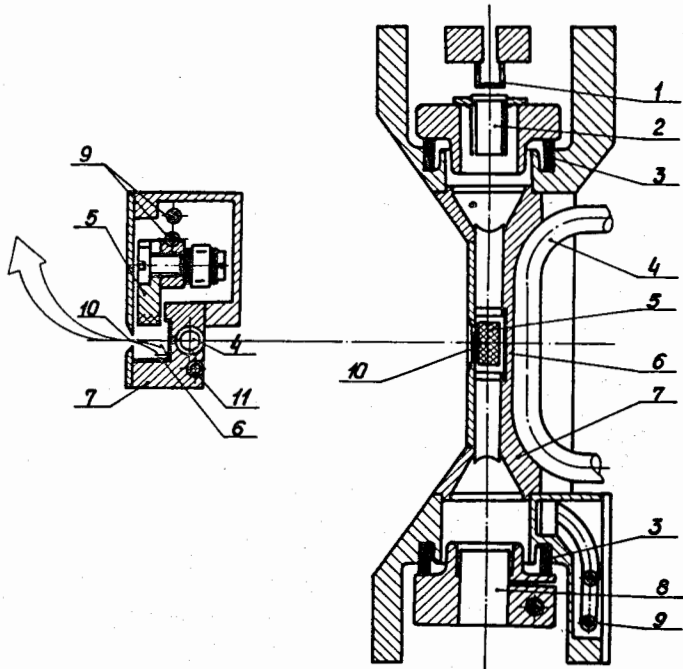


Fig.1 Schematic view of the ion source head: 1-filament; 2-cathode; 3-ring insulator; 4-cooling of the discharge chamber; 5-sputtering electrode; 6-insert for collection of sputtered material; 7-discharge chamber; 8-anticathode; 9-cooling of the sputtering electrode; 10-emission slit; 11-gas feed.

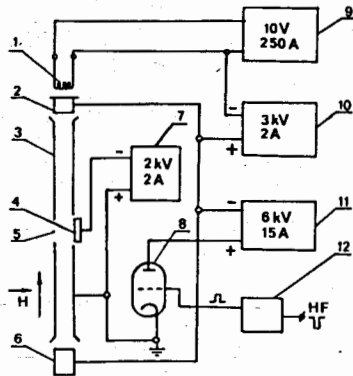


Fig.2 The diagram of the power supply circuit of the ion source: 1-filament; 2-cathode; 3-discharge chamber; 4-sputtering electrode; 5-emission slit; 6-anticathode; 7-sputtering electrode power supply; 8 and 12-modulator; 9-filament power supply; 10-cathode heating power supply; 11-discharge power supply.

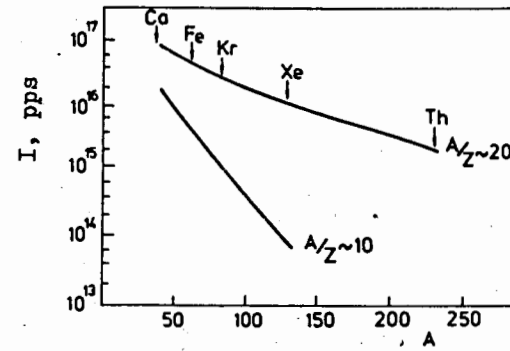


Fig.3 The yield of ions with mass to charge ratio $A/Z=10 - 20$ from the PIG source at test operation.

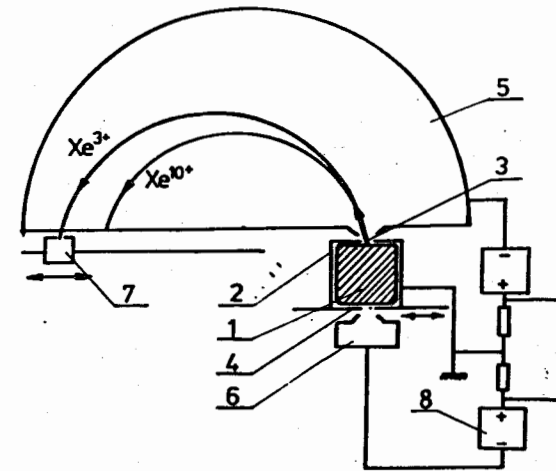


Fig.4 The scheme of extraction and analysis of the ion beam from the source with two emission slits: 1-plasma bulk; 2-discharge chamber; 3-emission slit; 4-movable plate with emission slit; 5-dee with extracting electrode; 6-extracting electrode-collector; 7-movable collector; 8-high voltage power supplies.

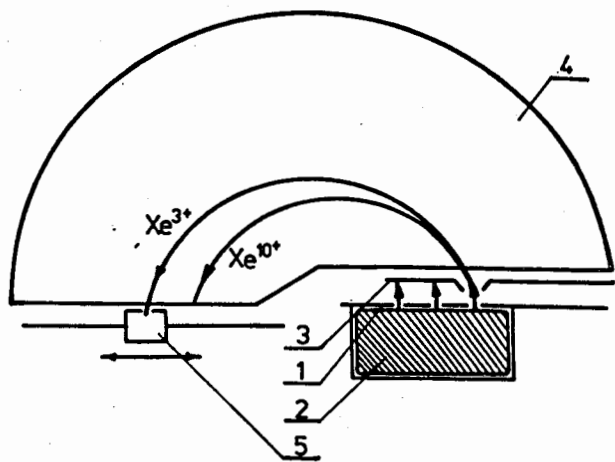


Fig.5 The scheme of extraction and analysis of the ion beam from the source with extended cathode and several emission slits: 1-movable plate with emission slits; 2-plasma bulk; 3-movable extracting electrode; 4-dee; 5-movable collector.

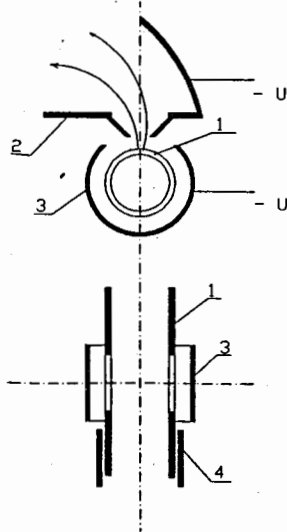


Fig.6 The scheme of extraction and analysis of the ion beam from the source with the circular emission slit: 1-discharge chamber; 2-dee with extracting electrode; 3-circular extracting electrode; 4-movable cylinder with a slit.

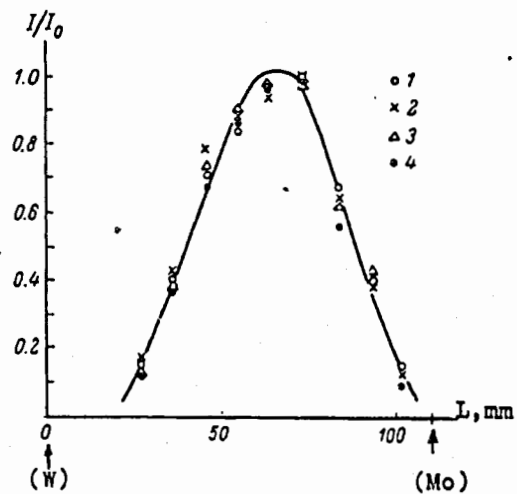


Fig.7 The distribution of the spectral lines ArI(1), ArII(2), ArIII(3), ArIV(4) intensities along the discharge. Arrows indicate the position of the cathode (W) and anticathode (Mo).

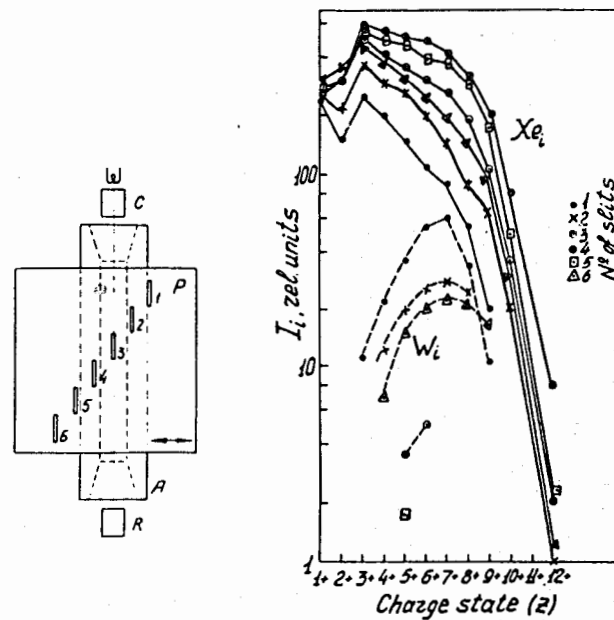


Fig.8 The scheme of the experiment (left) and charge state distributions of ion beams extracted through the slits 1 - 6.

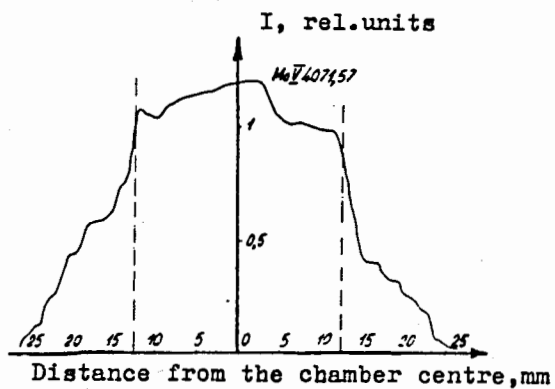


Fig.9 The distribution of MoV spectral line intensity along the discharge in the ion source with Mo sputtering electrode.

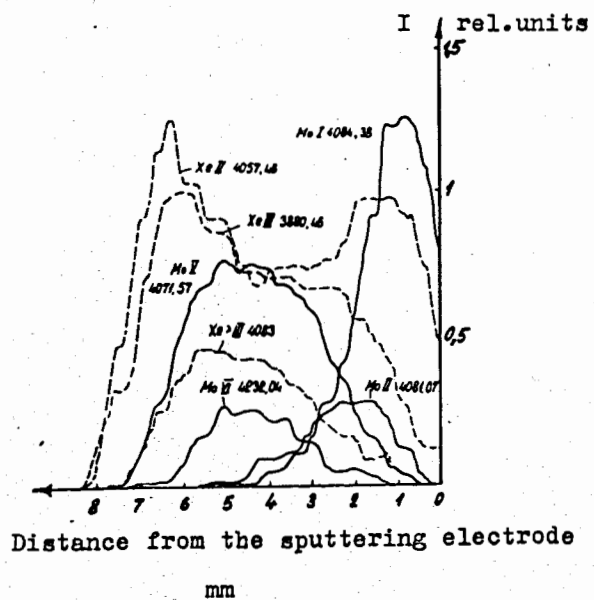


Fig.10 Transversal distribution of the Mo and Xe spectral lines intensity in the ion source with the Mo sputtering electrode and Xe as a support gas.

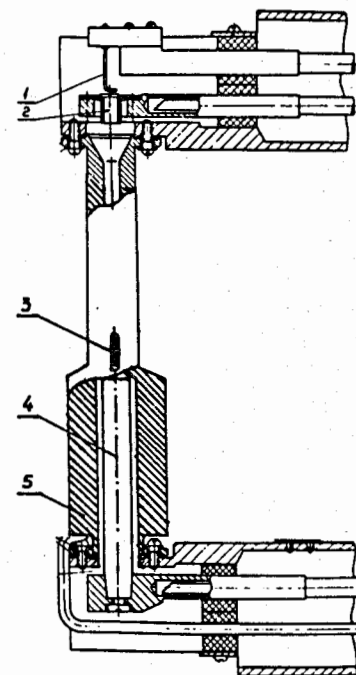


Fig.11 Schematic view of the ion source of intense ion beams of refractory metals. 1-filament; 2-cathode; 3-emission slit; 4-anticathode; 5-anode.

CONCLUSION

The PIG ion source with indirectly heated cathode is rather universal source for production of multiply charged ions of gases and solids. The results of experiments indicate the possibility of enlargement of the source emission surface with conservation of the charge state distribution of extracted ions.

The optimal conditions for the extraction of intense beams should be determined with taking into account of spatial distribution of discharge plasma components.

The design of the source for production of intense beams of multiply charged ions of refractory ions is proposed. The results of ion source tests indicate the higher yield of highly charged ions of Mo and W in comparison with the ion source with sputtering electrode.

REFERENCES

1. Yu.P.Tretyakov, V.B.Kutner, A.S.Pasyuk, S.L.Bogomolov, G.M.Solovjeva, In: Proc. of the VII All-Union Conference on Charged Particle Accelerators. Volume 1, p.81. JINR, Dubna, 1981 (in Russian)
2. V.B.Kutner, S.L.Bogomolov, A.A.Efremov, A.S.Pasyuk, Yu.P.Tretyakov, Rev. Sci. Instr. 1990, v. 61(1) part 2, p.p 487 - 489.
3. Bohm D. et al. The Characteristics of Electrical Discharges in Magnetic Fields. N.Y. 1949.
4. A.S.Pasyuk et. al., Pribori i tehnika eksperimenta 1965 N1, p.28-33 (in Russian)
5. Mavrogenes G.S., Ramler W.J., Turner C.B., IEEE Trans. on Nucl. Sci. 1965, v.NS-12, p.769
6. M.Muller, Z.Weijang, GSI Scientific Report, GSI-82-1, p.284
7. L.P.Kulkina, A.S.Pasyuk Zhurnal Tekhnicheskoi Fiziki, 1966, v.34, N4, p.726 (in Russian)
8. B.N.Makov IEEE Trans. on Nucl. Sci. 1976, v.NS-23, N2, p.1035
9. Yu.P.Tretyakov JINR P7-80-641, Dubna 1980 (in Russian)
10. N.P.Romanov, A.P.Striganov Optika i spektroskopiya, 1969, v.27, N1, p.17-24 (in Russian)
11. A.S.Pasyuk, Yu.P.Tretyakov, S.K.Gorbachev Atomnaya Energiya 1968, v.24, N1, p.21-25 (in Russian)

Received by Publishing Department
on March 18, 1996.